*33rd EPS Conference on Plasma Phys. Rome, 19 - 23 June 2006 ECA Vol.**30I**, P-2.074 (2006)*

Electron heating and plasma formation in a helicon discharge

M. Krämer, B. Clarenbach and K. Niemi

Institut für Experimentalphysik II, Ruhr-Universität Bochum, D-44780 Bochum, Germany

1. Introduction

The *rf* power absorption in the core of high-density helicon discharges has been shown to be intimately related to parametric excitation of electrostatic fluctuations [1]. Furthermore, it has been observed that the *rf* power carried by the helicon wave is absorbed by a nonlinear process thus evidencing that the energy is deposited in the plasma via the strongly damped short-scale fluctuations. In the present study, we investigated the *rf* power deposition, the electron heating and the plasma production focussing, in particular, on the spatial and temporal dependence of the relevant experimental parameters.

2. Experimental

The investigations were carried out on the helicon source HE-L (r_p = 73 mm, l_p = 1.1 m, τ_{pulse} = 2 – 4 ms, f_{pulse} = 25 – 100 Hz, $P_{rf} \leq$ 1.5 kW, f_{rf} = 13.56 MHz, m = 1 helical antenna coupling, $n_e \leq 2\text{x}10^{19}$ m^{-3}, $T_e \approx$ 3 eV, $B_0 \leq$ 0.1 T, p = 0.3 – 1.0 Pa argon gas [2]). Optical emission spectroscopy (OES) was applied to determine the electron temperature with the aid of a collisional-radiative model. In addition, Langmuir probes were used to measure the electron temperature and density. The fluctuations of the density were detected with the same probe while the *rf* magnetic field of the helicon wave was picked up with a B-dot probe.

3. Results

A characteristic feature of helicon discharges with helical antenna coupling is the predominant excitation of the m = +1 helicon mode leading to a pronounced axial asymmetry of the *rf* power deposition with respect to the antenna. A typical quasi-snapshot of the helicon wave field amplitude has been plotted in Fig.1a. It is seen that helicon waves (m = +1 modes travelling in $\mathbf{B}_0$ direction) are excited only on one side of the antenna. Apart from the fraction of the field energy concentrated close to the antenna due to direct inductive coupling (z ≈ 8 - 10 cm) the *rf* field energy and the *rf* power absorption is largest on the axis. (Note the small modulation of the amplitude with $\lambda_z/2$.) This energy fraction which is only associated with the m = +1 mode accounts for the plasma production in the centre of the discharge. As a result, the electrostatic fluctuations excited by the helicon wave have their maximum in the centre as well (Fig.1b). These fluctuations, which were identified as ion-sound and Trivelpiece-Gould

fluctuations originating from a parametric decay instability, carry the *rf* energy which is finally strongly absorbed [1].

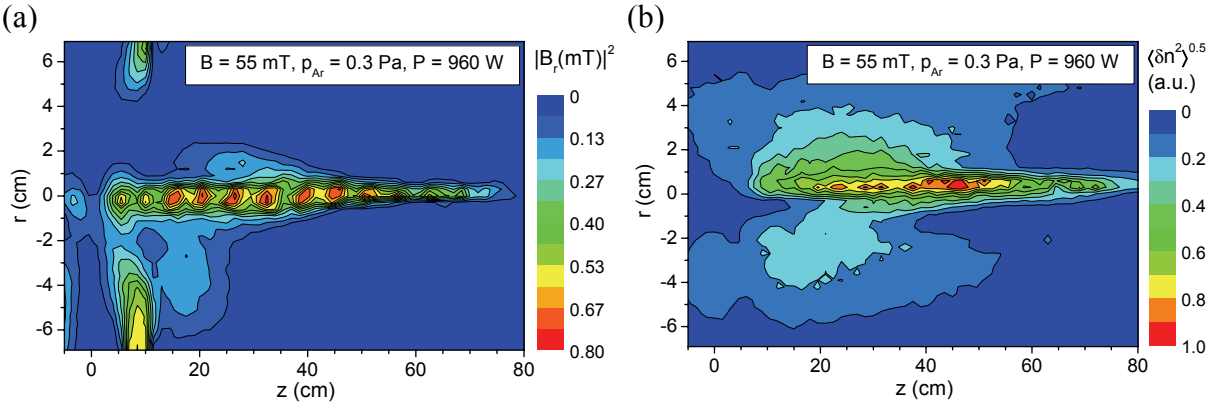

Fig1: Contour plots of the rf magnetic field energy (a) and density fluctuation amplitude (b) for the m = +1 side (centre of antenna at r = z = 0).

The asymmetry of the *rf* power deposition can also be seen from the radial profile of the ArII line intensity (Fig.2). Since it scales with n_e^2, we also plotted the square of the ion saturation current. Indeed, the line emission on the m = -1 side follows the n_e^2 curve thus proving T_e = *const.* over the radius. However, on the m = +1 side of the antenna, we observe a pronounced peak on the axis (*blue core*) thus indicating significant electron heating.

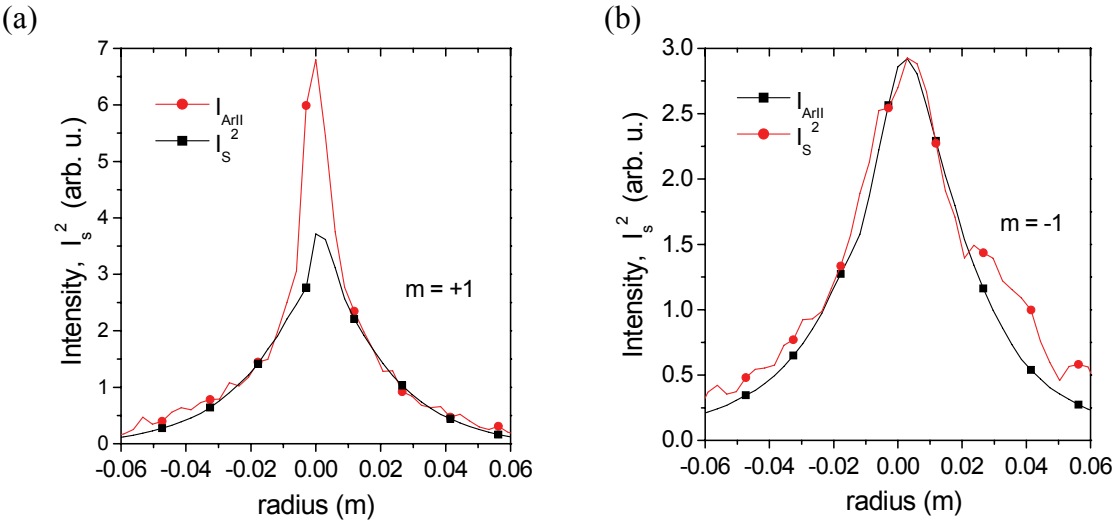

Fig2: Radial profile of the 480.6 nm argon ion emission and the squared ion saturation current 25 cm away from the centre of the antenna for the m = +1 (a) and m = –1 side (b) (B = 54 mT, P = 0.2 Pa, P = 1.4 kW).

This is also in agreement with probe measurements showing a peaked profile of T_e in the centre (Fig.3). The temperature growth towards the plasma edge can be attributed to heating by inductive fields near the antenna windings. The shape of the density profile which is much broader can be explained by assuming the plasma to be produced only by a line source on the axis (blue line). Although T_e increases at the plasma edge, the thermal energy density has a

pronounced maximum only on the axis as shown in Fig.3b. We also plotted the magnetic energy density and the fluctuation amplitude which exhibit even much narrower profiles. Obviously, the conductive and/or convective heat transport across $\mathbf{B}_0$ is significant.

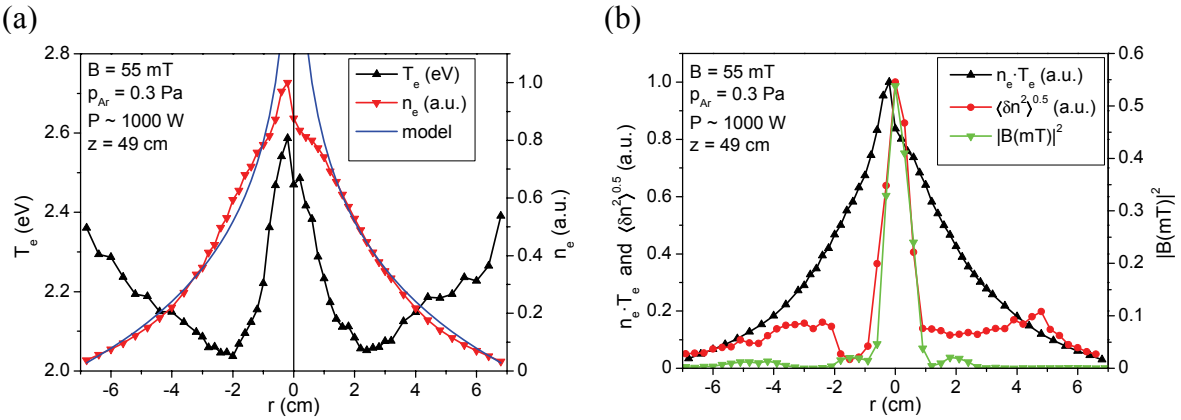

Fig3: Profiles of electron density and temperature (a) and thermal energy density, magnetic energy density and fluctuation amplitude (b) 49 cm away from centre of antenna.

To measure the electron heating rates we applied a double pulse technique, i.e., a high-power pulse ($P_{rf} \approx 1$ kW) producing the plasma was followed by a second pulse of variable *rf* power with 20 – 30 µs delay. We thus get a target plasma of low temperature enabling us to study the growth of T_e in the high-density plasma starting at low values in the second *rf* pulse.

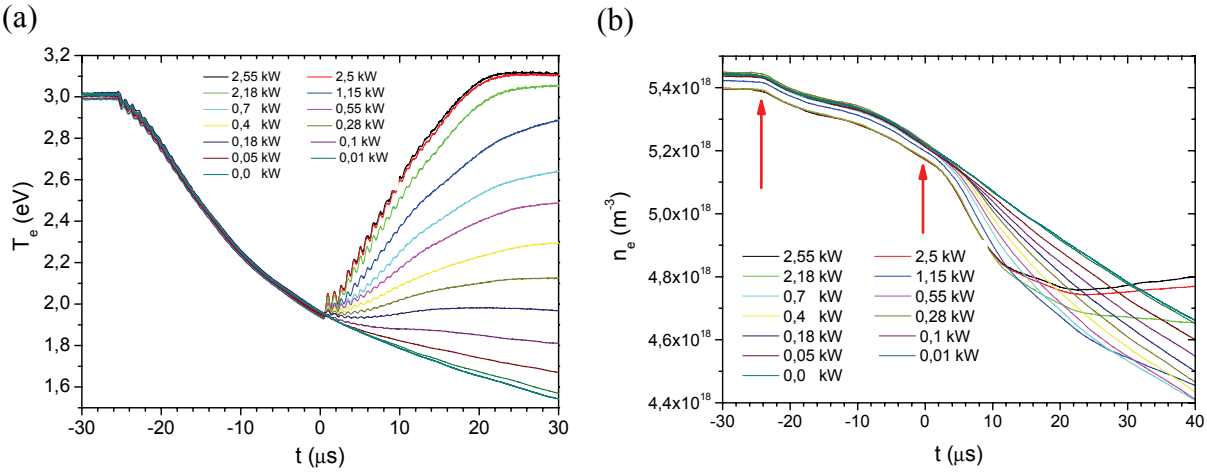

Fig.4: Evolution of the electron temperature (a) and density (b) during the double rf pulse for different rf powers (pause 22 µs, B = 40.5 mT, P_{Ar} = 0.3 Pa, P = 1.4 kW, z = 25 cm).

Fig.4 shows the temporal behaviours of the electron density and the electron temperature for different *rf* powers in the second pulse. It can be seen that the density profile remains nearly constant thus allowing helicon wave propagation from the beginning of the second pulse. At the end of the first *rf* pulse, the temperature decreases very fast and reaches a sta-

tionary value (original value in case of equal *rf* power) at about 20 μs after the beginning of the second pulse.

The electron temperature obtained from OES and Langmuir probe measurements was observed to grow proportionally to the *rf* power in the second pulse. From the growth of T_e in the first few μs (only probe measurements in Fig.4a), we calculated the electron heating rates being proportional to the *rf* power. Hence, we conclude that there is no threshold *rf* power, that is, irrespective of the helicon wave absorption mechanism, the electrons are heated by collisional processes. The local electron heating scales with the axial damping decrement k_{zi} of the helicon wave yielding the absorbed power per length $2k_{zi}P(z) \cong 3\pi a^2 n_{e0} k_B \dot{T}_e / 2$, if $n_e(r) = n_{e0}\exp(-r^2/a^2)$ and $T_e(r)$ = *const*. From the measured k_{zi} = 4.5 m^{-1} and $P_{rf} \approx$ 500 W, a = 26 mm, $n_{e0} = 10^{19}$m^{-3} we find $\dot{T}_e \cong$ 0,9 eV / μs which is too large. However, due to the large parallel heat conductivity and the axially asymmetric power deposition, it is reasonable to assume the thermal energy to be equally distributed over half the plasma length, $L \approx$ 0.5 m leading to $P = 3\pi a^2 L n_{e0} k_B \dot{T}_e / 2$ and $\dot{T}_e \cong$ 0,2 eV/μs in agreement with the measured value.

The evolution of the electron density in the second pulse can be described by the diffusion equation. Due to the strong magnetic confinement, cross-field diffusion can be neglected compared to parallel diffusion leading to $\partial n_e / \partial t \cong R_{ion}(T_e) n_g n_e - D_{a\parallel} \nabla^2 n_e$ (R_{ion}: ionisation rate, $D_{a\parallel} = k_B T_e / m_i \nu_{in}$). At small *rf* powers, the electron heating leads to enhanced diffusion. For sufficiently high temperature, the ionisation exceeds the diffusion losses and the density increases. Good agreement between the measured and calculated density curves is achieved if the diffusion length is assumed to be given by the discharge length, $\Lambda = l_p / \pi$ ($l_p \approx$ 1 m).

3. Conclusions

The present observations have shown that the *rf* power in a high-density helicon discharge is predominantly carried by the m = +1 helicon mode and deposited in the narrow core around the tube axis in which turbulent fluctuations are excited. As a result, electron heating occurs only close to the axis. The remaining regions of the helicon plasma can reasonably be understood in terms of particle and energy transport along and across the magnetic field.

Acknowledgements: This work was supported by the *Deutsche Forschungsgemeinschaft* through the Sonderforschungsbereich 591 (Project A7).

[1] B. Lorenz, M. Krämer, V. Selenin, Yu. Aliev, Plasma Sources Sci. Techn. 14, 623 (2005).
[2] M. Krämer, B. Lorenz, B. Clarenbach, Plasma Sources Sci. Techn. 11A, 120 (2002).